Supplementary Information file for

Which is a Better Fluorescent Sensor: Aggregation-Induced Emission-Based Nanofibers or Thin-Coating Films?

Yexin Ding, Weili Li, Fangming Wang, Hongkun Li, Shengyuan Yang, Lijun Wang, Zhiming Wang, Mike Tebyetekerwa*, and Ben Zhong Tang**

This file contains

Experimental section

Supplementary notes 1-6

Figures S1-7

Tables S1-2

Schemes S1-3

Supplementary information references

The file is 13 pages

Experimental

Materials

Methyl methacrylate (MMA), 2-ethylhexyl acrylate (2-EHA), hydroxyethyl acrylate (HEA) and benzoyl peroxide (BPO) were all purchased from Sinopharm Chemical Reagent Co. Ltd (≥99.0%). All the acrylic monomers were purified by reduced pressure distillation. Butyl acetate, dichloromethane (DCM) and N'N-dimethylformamide (DMF) were obtained from Jiangsu Qiangsheng Functional Chemistry Co. Ltd (≥99.9%). Dicyclohexylcarbodiimide (DCC）was provided by Wuxi Prospect Chemical Reagent Co. Ltd (≥99.0%). TPE-4COOH was synthesized in our laboratory according to the reference [1] and steps provided in *Supplementary note 2* (^{1}H NMR (DMSO-d^6, 300 MHz): δ= 7.11-7.13 (d, 8 H), 7.73-7.75 (d, 8 H), 12.97 (s, 4 H) ppm.). Deionized water was specially prepared in our laboratory.

Characterization and methods

^{1}H NMR was measured on Bruker ARX 400 NMR spectrometers by using DMSO-d^6 as the deuterated solvent and tetramethylsilane (TMS;δ=0 ppm) as the internal standard. FTIR spectra were recorded on a Perkin-Elmer 16 PC FTIR spectrophotometer. Thermogravimetric analysis (TGA) measurements were carried out under nitrogen on a Perkin-Elmer TGA 7 analyzer at a heating rate of 10 C min^{-1}. Relative number molecular weight (Mn) of the obtained resins was estimated by a Waters Associates gel permeation chromatography (GPC) system equipped with RI and UV detectors. THF was used as eluent at a flow rate of 1.0 mL/min. Images of scanning electron microscopy (SEM) were taken on a JSM-6700F electron microscope. X-ray diffraction (XRD) measurements were performed using an XRD diffraction (D-MAX 2200 VPC) equipped with Ni-filtered Cu/Ka radiation, having a wavelength of 0.154 nm. Fluorescence spectra were recorded using a steady states spectrometer (Spectrofluorometer FS5, Edinburgh Instruments) equipped with a temperature control system (Oxford Instruments).

Supplementary note 1. Synthesis of different acrylic resins

In a standard preparation process, MMA, 2-EHA, HEA, BPO and butyl acetate were selected as the hard monomer, soft monomer, functional monomer, thermal initiator and solvent, respectively. Table S1 lists the relative content of reactants, and Scheme S1 describes the reaction equation to synthesize the acrylic resin. In a standard polymerization process, the blended monomers and initiator were mixed up and dropped into butyl acetate and stirred at 110 ℃ for 3 hrs under nitrogen atmosphere. After that, the mixture was kept at 120 ℃ for 3 hrs to obtain the acrylic resin. DSC results (Figure S1) indicated that T_g values of the obtained acrylic resins were close to the theoretical design values, and GPC results in Figure S2 demonstrates that M_n of acrylic resins decreased with the enhanced content of initiator, which are in accord with the principle of free radical polymerization.

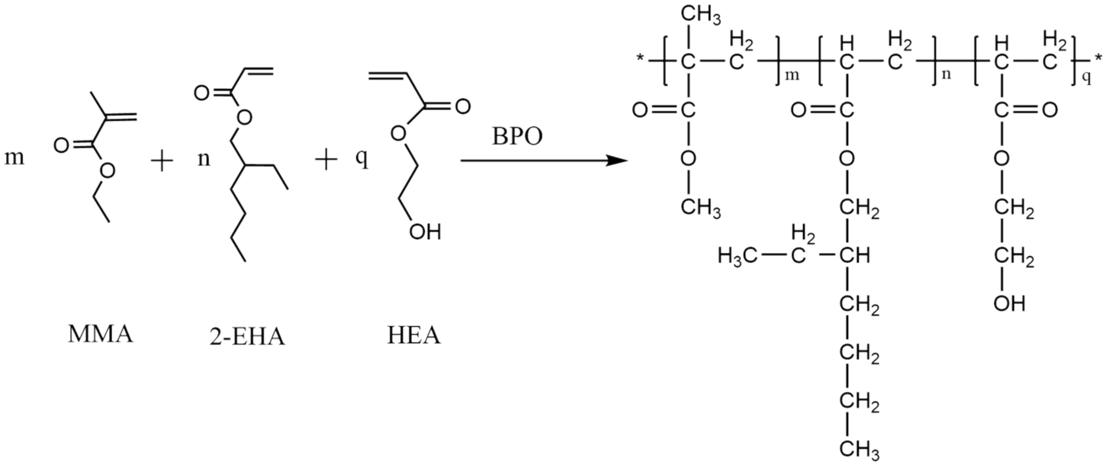

Scheme S1. Synthesis of acrylic resin

Table S1. The series of acrylic resins synthesized

Sample	Monomer ratio (MMA/2-EHA/HEA)	Initiator content（wt%）
AR-1	0.398/0.397/0.205	0.6
AR-2	0.516/0.279/0.205	0.6
AR-3	0.618/0.177/0.205	0.6
AR-4	0.708/0.087/0.205	0.6
AR-5	0.618/0.177/0.205	0.45
AR-6	0.618/0.177/0.205	0.75
AR-7	0.618/0.177/0.205	0.9
AR-8	0.618/0.177/0.205	1.05

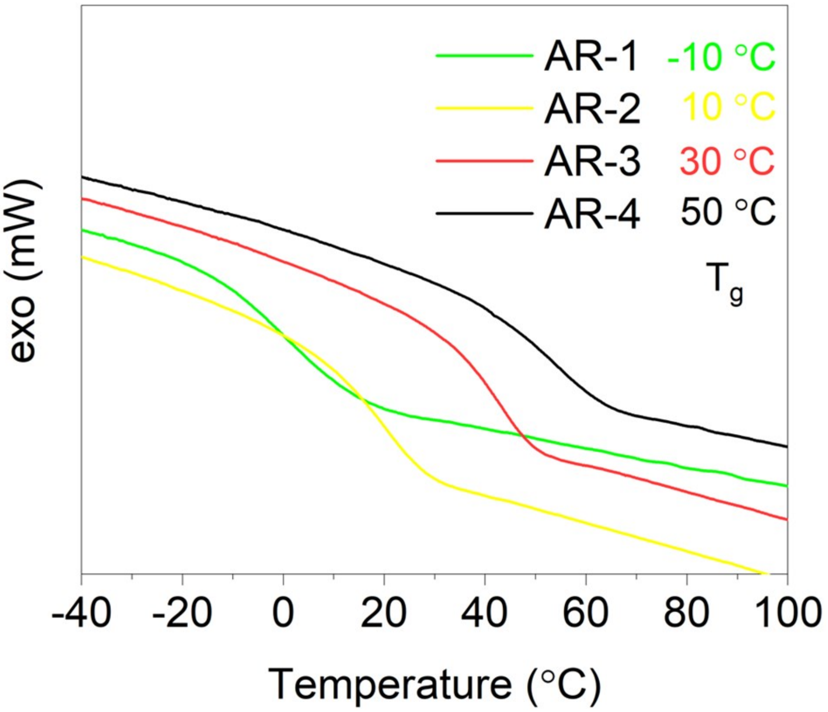

Figure S1. DSC curves of the synthesized resins with their Tg values.

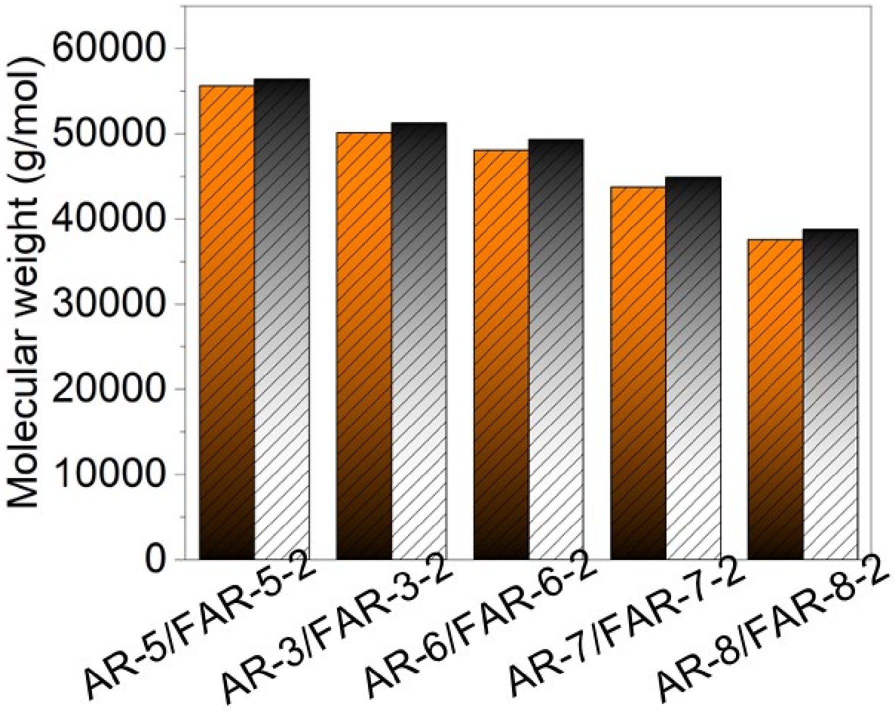

Figure S2. GPC histograms of the different ARs as their varied initiator content.

Supplementary note 2. Synthesis of the AIEgen

The Synthesis of the AIEgen proceeded according to Scheme 1. First, TPE (6.648g, 0.02 mol) was dissolved into CH_2Cl_2 (300 ml), the blended solution was dipped into bromine (19.2 g, 0.02 mol), then the reaction was left to proceed for 2 days. When the reaction was terminated, the resultant product was placed in ice water and neutralized with sodium hydroxide solution to eliminate the unreacted bromine. After extraction process, the obtained TPE-4Br was left in the organic liquid. By removing the organic liquid (CH_2Cl_2), the pale yellow wax of TPE-4Br was obtained and purified through recrystallization process, its yielded was 4.147 (32 wt%). Then, the Sandmeyer reaction between TPE-4Br and CuCN in N,N-Dimethylformamide (DMF) was performed to attach the CN moieties onto TPE. To a 100 mL two-necked round-bottomed flask, TPE-4Br (3 g, 4.63 mmol), CuCN (2.37 g, 26.4 mmol) and anhydrous DMF (45 mL) were added. The mixture was heated at 160 ℃ for 3 days, and then cooled down to 90 ℃. Subsequently, ethylenediamine (10 mL) and H_2O (15 mL) were added into the mixture and heated to reflux for 3 hrs. After cooling down to room temperature, TPE-

4CN was obtained by extracting with dichloromethane (DCM) and drying over anhydrous magnesium sulfate. After filtration and solvent evaporation, crude TPE-4CN underwent hydrolysis reaction carried out in ethylene glycol (60 mL) containing NaOH (0.8 g, 20 mmol) at 200℃ for 3 days. Then, HCl (1 mol/L, 20 mL) solution was added carefully to quench the reaction after cooling down to room temperature. Pale brown solid of TPE-COOH was yielded 0.988 g（42 wt% yield）after filtering, washing with water for three times and air drying. ^{1}H NMR (DMSO-d^6, 300 MHz): $\delta = 7.12$ (d, 8 H), 7.74 (d, 8 H), 12.97 (s, 4 H) ppm.

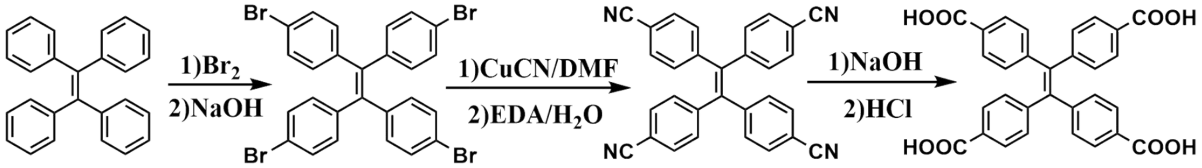

Scheme S2. Synthesis procedure of the tetracarboxylic-tetraphenylethylene (TPE-4COOH) AIEgen

Supplementary note 3. Synthesis of the polymer-AIEgen

In the 50 mL round-bottom flask, TPE-4COOH (of different amount 0.05-2 wt%) and acrylic resin (AR-3) in butyl acetate at RT conditions under nitrogen were mixed together. After all the solids were dissolved, DCC was added. The reaction mixture was allowed to warm to room temperature and stirred for 24 hrs under nitrogen atmosphere. The resultant suspension was then filtered. After filtration, the filtrate was added dropwise into petroleum ether under vigorous stirring to obtain the resultant product. To obtain the fluorescent acrylic resin (FAR), the resultant product was then isolated by filtration and dried in vacuum at 40 °C overnight. The general reaction equation of obtaining FAR is shown in Scheme S3. Figure S3 presents FTIR spectra of acrylic resin, FAR and TPE-4COOH. Also, comparative T_g data of the acrylic resin and the new obtained FAR is plotted in Figure S4

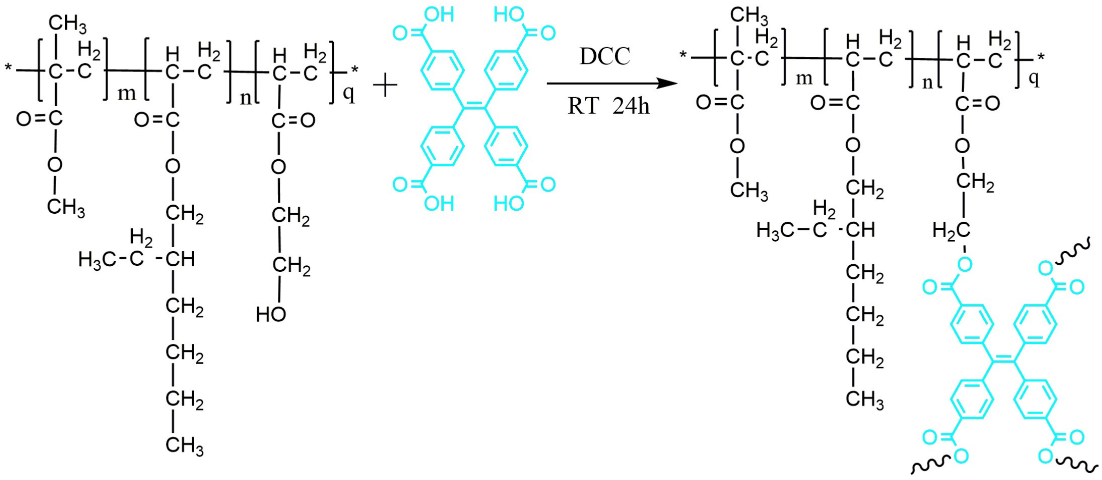

Scheme S3. Synthesis of fluorescent acrylic resin (FAR)

Table S2. The series of Polymer-AIEgen materials synthesized

Sample	Monomer ratio (MMA/2-EHA/HEA)	Initiator content（%）	Relative content of TPE-4COOH（%）	Relative content of DCC（%）
FAR-3-0.05	0.618/0.177/0.205	0.6	0.05	0.1
FAR-3-0.1	0.618/0.177/0.205	0.6	0.1	0.2
FAR-3-0.5	0.618/0.177/0.205	0.6	0.5	1
FAR-3-1	0.618/0.177/0.205	0.6	1	2
FAR-3-2	0.618/0.177/0.205	0.6	2	4

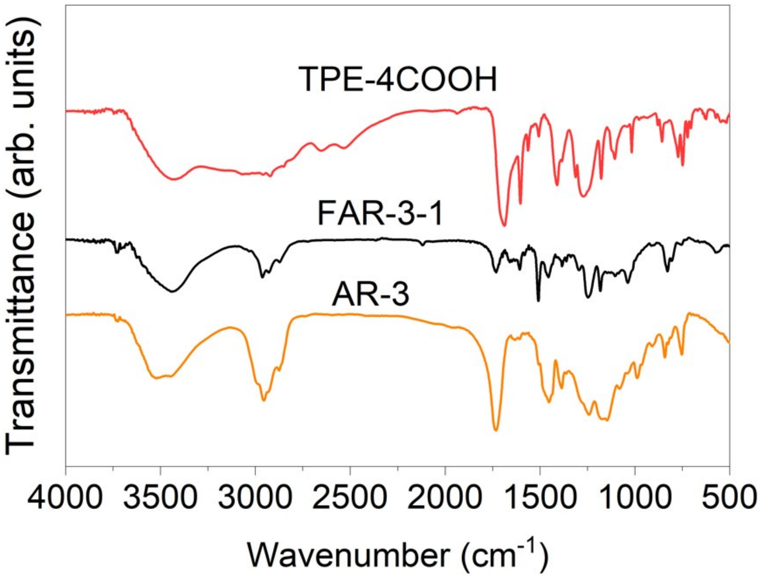

Figure S3. FTIR spectra of acrylic resin, FAR, and TPE-4COOH AIEgen. Notably, the peaks at 1607 cm^{-1}, 1581 cm^{-1}, 1509 cm^{-1} and 1456 cm^{-1} for FAR can be assigned to the benzene rings, which are attributed to the characteristic absorption peak positions of TPE-4COOH. The results indicated that AIEgen was successfully grafted into the acrylic resin.

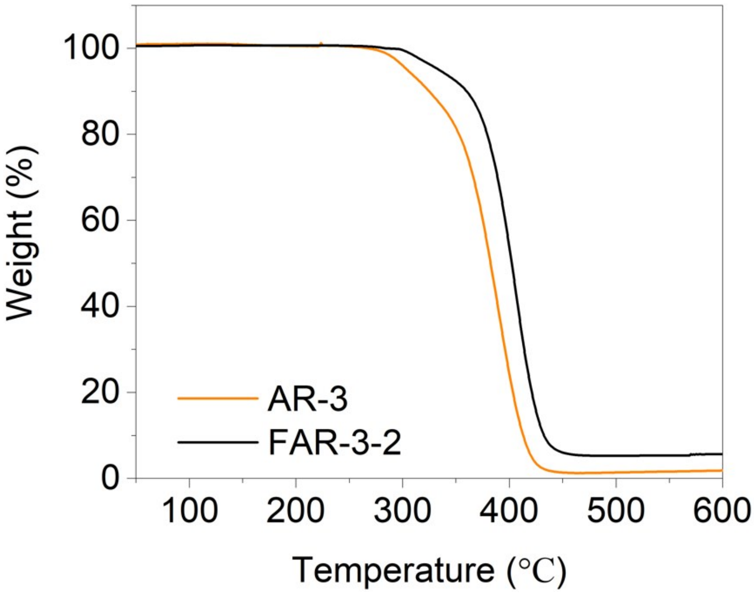

Figure S4. TGA curves of acrylic resin (AR-3) and fluorescent acrylic resin (FAR-3-2). The decomposition temperature of acrylic resin and FAR are around 290 ℃ and 300 ℃, respectively. The increased molecular weight and the partial crosslinking structure of acrylic resin with the knitted TPE-4COOH explain the slight improvement in the thermotolerance of the FAR. This makes the final FAR material stable enough to be applied in our intended applications of probing the changes in the environmental conditions.

Supplementary note 4. Control of the associated reactions and synthesis of materials

Based on the traditional characterization techniques, it is difficult to monitor the polycondensation reaction process in real-time, not to mention determining the termination point. However, according to the restriction of intramolecular rotation mechanism, the intramolecular rotation of AIEgen rotors is related closely with the surroundings-thus AIEgen's emission. The emitted light from the AIEgen (or its composites) can thus be utilized track the reaction process according to our research results.[1,2] Taking an example the FAR system (FAR-3-2) in Figure S5, the peak position shifts in a different manner with varying intensities. For the FAR in solution, the PL peak shifts from 470 nm to 490 nm (and then stabilizes) with the reaction time of above 24 hrs (Figure S5A and B). The observation of fluorescence spectrum becoming stable (position and intensity) signifies reaction termination. Consequently, this time was recorded for all further experiments and used as the total reaction time for reproducibility of the results.

Similarly, the whole drying process of FAR can also be traced in real-time with this approach. Generally, the formed chemical bonds are known to restrict the intramolecular rotation of TPE molecular rotors and lead to the enhancement of the sample's fluorescence intensity (as observed in Figure S5C and D). This clearly explains why we see a rapid fluorescence intensity rise within just ~3 min for the AIE in the acrylic polymer system during the drying process. Besides, the redshift can be attributed to the surrounding polymer chains which increase the polarity of the system.[3]

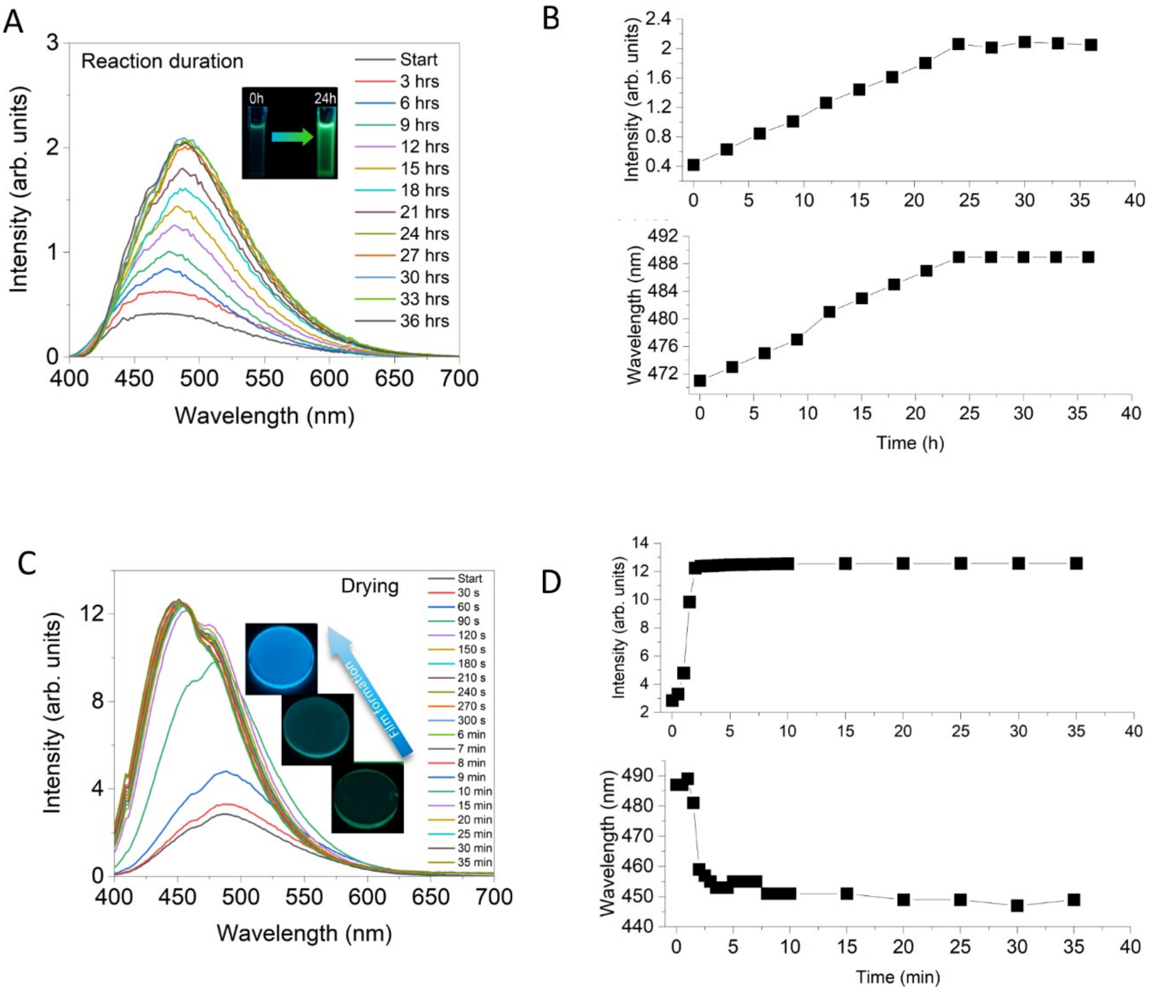

Figure S5. Reaction duration: (A) Fluorescence spectra of FAR and (B) analysis of how its PL peak position and intensity varied with reaction time (~36 hrs). Drying duration: (C) Fluorescence spectra of FAR and (D) the peak position and fluorescence intensity with drying time (~35 min). Inset are real images of the samples under UV light source (365 nm). The strong fluorescence in (C) means that the AIEgen was successfully knitted with the polymer chains via the chemical bond.

Supplementary note 5. Preparation of electrospun fluorescent nanofibers (FNFs)

First, different spinning solutions were obtained by dissolving the synthesized FAR into DMF with its concentration being set at 25 w%t. Then, electrospinning was done on JDF05 electrospinning apparatus (Changsha Nayi Instrument Technology Co., Ltd, Changsha, China). The FNFs were collected by a metal cylinder collector wrapped with aluminium foil kept at a fixed distance of 15 cm away from the needle tip of the spinneret. The spinneret had an inner diameter (ID) of 0.90 mm and an outer diameter (OD) of 1.20 mm. The spinning voltage was adjusted to 10 kV, and the spinning fluid flow rate was adjusted to 1 mL/h. After finishing the electrospinning process, the obtained FNF membranes were then dried in a vacuum oven at 25 ℃ for 12 hrs to ensure the complete volatilization of the solvent. For comparison, a flat coating based on the same fluorescent acrylic resin was also prepared by spinning coating.

Supplementary note 6. Factors dictating the nature of FNFs.

Factors affecting the properties of the resultant fibers such as morphology, surface area, diameter, porosity, *etc.* were first probed. Before we obtained the optimum FNFs, the spinning parameters (*Supplementary note 5)* were followed, and the weight content of TPE-4COOH was set at 2 wt% (the relative AIEgen percent which provided the best emission (Figure. S7)). Then we systematically studied the effect of T_g value and the molecular weight (M_n) of acrylic resin on the morphology of the FNFs.

According to Figure S6A, FNFs from FAR having theoretical T_g values of -10 ℃ could be obtained at very low viscosity of 71mPa·s at room temperature and were soft with thick rubbery morphologies. When the T_g value of FAR was increased, the diameter of the obtained nanofibers got thinner. Moreover, when the T_g value of FAR was 30 ℃, the nanofibers showed uniform and excellent morphologies, which could be obtained at the viscosity spinning speed of 332 mPa·s at room temperature (these conditions here were utilized in the proceeding experiments). More still, when the T_g value of FAR rose to 50 ℃, the required spinning viscosity was raised to 405 mPa·s at room temperature. In this FAR, the rigid polymer chains led to the spinning solution not being split/ stretched well while being ejected in high voltage field. So massive big bead appeared in the obtained thin FNF mats.

Now T_g value was set at 30℃ and FAR with different M_n was utilized. According to Figure S6B, when M_n of FAR was set to 38700 g/mol, no FNFs could be realized except large string beads. With the M_n of FAR increasing, the FNFs progressively started to form, and the beads on the nanofibers gradually are dwindled. When the M_n reached 51200 g/mol, the viscosity of the spinning solution increases to 332 mPa·s at room temperature, which could present FNFs having a smooth shape with a uniform diameter (optimum conditions). However, with further raise in M_n, the spinning viscosity also increased to solution 516 mPa·s at room temperature, and the size of the nanofibers started to increase. To summarize the results, with the M_n increasing, the morphology of membrane changes from microsphere to the nanofiber, along with the fiber diameter increasing.

Overall the optimum condition for the best-suited FNFs included, using FAR having T_g of 30 °C, with an acrylic resin having M_n of 51200 g/mol and the spinning viscosity of 332 mPa·s at room temperature.

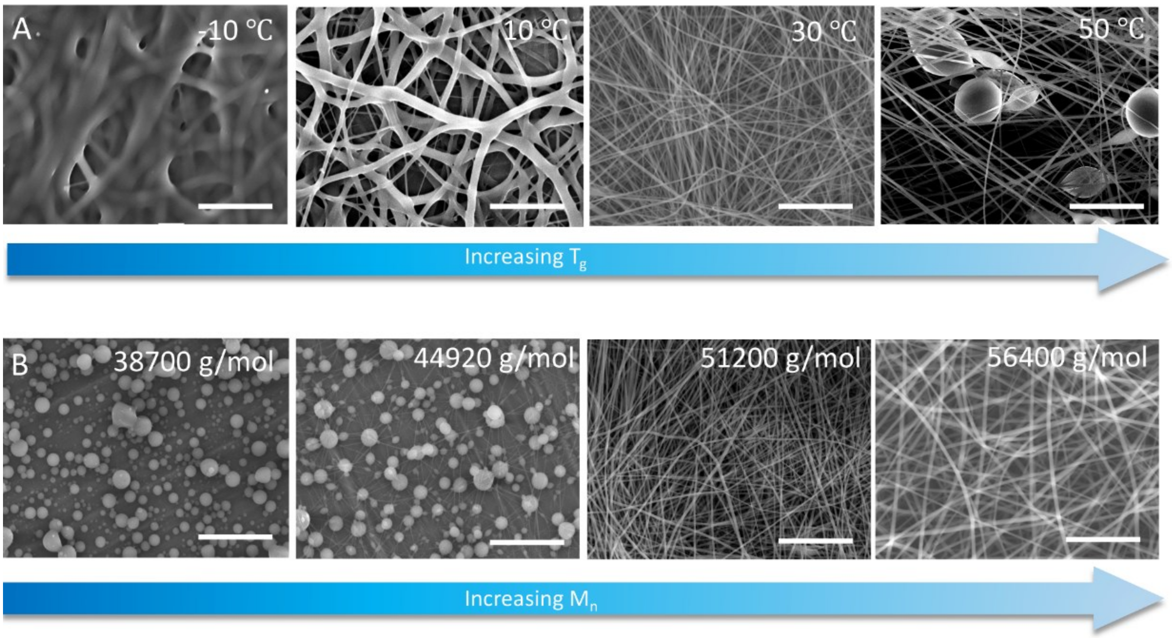

Figure S6. SEM image analysis of FNFs obtained with different conditions. (A) With different Tg of the FAR and (B) with different molecular weight of the acrylic resin (scale bar is 30 µm).

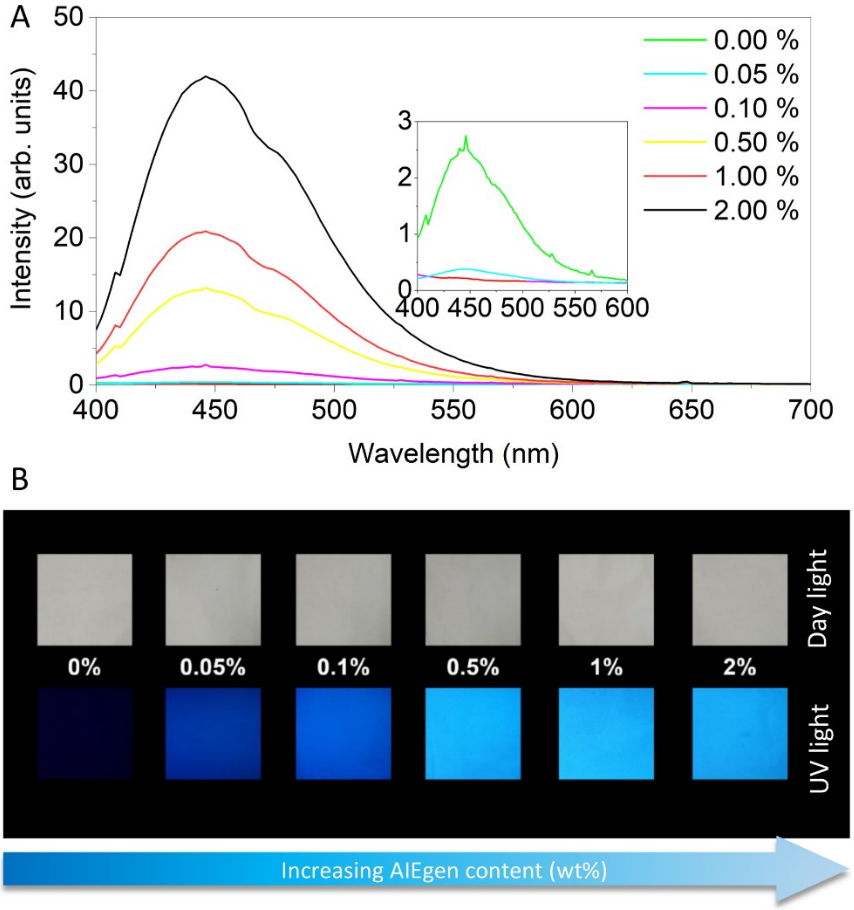

Figure S7. (A) Fluorescence spectra of the FNFs with respect to the change in TPE AIEgen doping percentages and (B) the corresponding optical images and UV-light (365 nm).

Supplementary Information references.

1. W. Yao, M. Tebyetekerwa, X. Bian, W. Li, S. Yang, M. Zhu, R. Hu, Z. Wang, A. Qin and B. Z. Tang, *J. Mater. Chem. C*, 2018, 6, 12849-12857.

2. W. Li, Z. Qiu, M. Tebyetekerwa, J. Zhang, Y. Wang, T. Gao, J. Wang, Y. Ding and Y. Xie, *Prog. Org. Coat.*, 2019, 127, 8-15.

3. R. D. Schaller, L. F. Lee, J. C. Johnson, L. H. Haber, R. J. Saykally, J. Vieceli, I. Benjamin, T.-Q. Nguyen and B. J. Schwartz, *J. Phys. Chem. B*, 2002, 106, 9496-9506.